
Pore Structure Change due to Calendering and its Effect on Ink Setting Behaviour – Review and Novel Findings

Peter Resch¹, Wolfgang Bauer² and Ulrich Hirn²

¹Sappi Austria Produktion GmbH & Co. KG, Brucker Straße 21, 8101 Gratkorn, Austria

²Graz University of Technology, Inst. of Paper, Pulp and Fibre Technology, Kopernikusgasse 24/II, 8010 Graz, Austria

ABSTRACT

Pore structure of the coating layer has a major impact on surface appearance, optical properties and printability performance of multiple coated papers. Generally fast ink setting can be realised by use of fine pigments as well as pigments with steep particle size distribution. Also ink-paper interaction of coated papers changes significantly by calendering.

Objective of this study was to generate fundamental knowledge regarding the influence of calendering on the pore structure of multiple coated papers and to highlight the impact of this pore structure change on ink setting behaviour. Calendering trials demonstrated that the pore structure of the calendered paper shrinks stepwise with increased calendering temperature. Mercury porosimetry and image analysis of SEM pictures of calendered papers highlighted that the gradual reduction of total pore volume in combination with the reduced surface porosity actually results in slower ink setting behaviour. In order to reach a desired paper gloss level, calendering with lower surface temperature and a higher number of nip passes is proposed if ink setting speed is to be preserved.

The obtained results were compared with common theoretical models for liquid penetration. These theoretical models are appropriately describing the influence of calendering induced pore structure changes on ink setting.

INTRODUCTION

As published by FOGRA in the annual report 2006, 35% of their expertises regarding complaints in sheet-fed printing were related to ink scuff and poor ink rub resistance, followed by ink setting and ink drying problems with 21% [1]. The increasing amount of complaints related to ink-setting, ink drying and ink rub resistance problems is caused by the demands for economic efficiency and profitability. Modern printing presses allow an increase in printing speed, which - in combination with shorter set-up times and less time between printing and converting - leads to the problems mentioned above.

As highlighted in previous publications [2, 3], finer pigments generally result in a coating layer that contains finer pores. *Figure 1* demonstrates that this relationship is more significant for precipitated calcium carbonates (rhomohedral and aragonitic PCC's) compared to ground calcium carbonates (GCC). At the same time, PCC generates larger pores compared to GCC with the same mean particle size. The main explanation for this finding is the typically steeper particle size distribution of precipitated calcium carbonates (PCC) compared to ground carbonates (GCC). For pigments with a steeper particle size distribution, fewer fines are available that could fill the voids being formed by coarser particles, while pigments with broader particle size distribution favour packing.

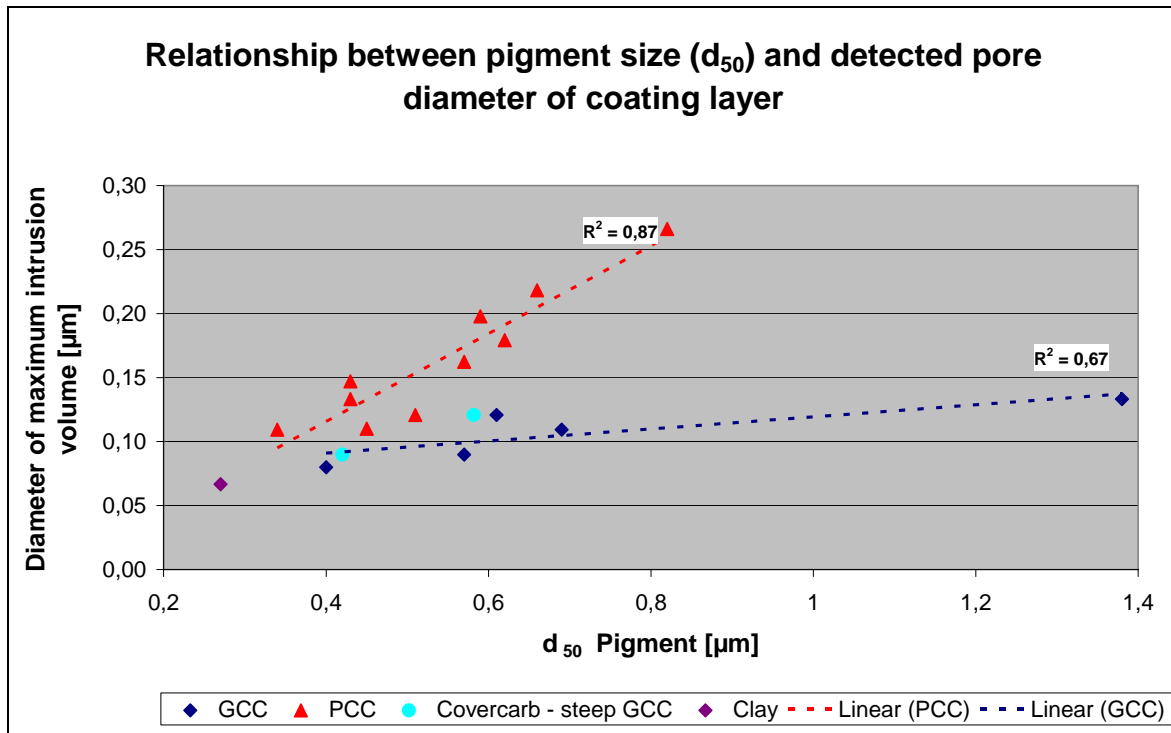


Figure 1 Relationship between pigment size and typical pore diameter of the applied coating layer [3]

As concluded in several publications, the coating structure of the top coat is the dominating effect determining the interaction of coated end paper with offset inks, paper gloss as well as smoothness, refer for instance to KOSSE ET AL. [4] and DONIGIAN [5].

In general, the ink-paper interaction of coated papers changes significantly by calendering. Objective of this study was to generate a better understanding and knowledge regarding the influence of calendering on the pore structure of multiple coated papers as well as to highlight the impact of this pore structure change on the ink setting behaviour of the calendered paper.

In this study uncalendered (woodfree) triple coated papers produced on a commercial paper machine were finished using a laboratory calender. Calender temperature, number of nip passes and line load were varied to find the optimum balance between paper gloss and set-off behaviour. The pore structure of the whole paper was analysed via mercury porosimetry and the surface porosity was assessed by evaluation of high resolution SEM pictures.

Gathered results of this investigation were compared with the outcome of the common theoretical models describing the impact of the pore structure of coated papers on the ink vehicle absorption.

Models describing the impact of pore size on fluid penetration into the porous structures

In this first section, an overview about the paper related models to describe the fluid penetration into pore structures by equations is given.

In the used equations the following abbreviations are used:

| | |
|---------------|-------------------------------|
| V_p | Penetration volume |
| x | Penetration depth |
| t | Time |
| R | Pore radius |
| $R_{pigment}$ | Radius of pigment particle |
| n_p | Number of pores per unit area |
| η | Viscosity |
| γ | Interfacial tension |

| | |
|----------------------|--|
| θ | Contact angle |
| K | Darcy coefficient |
| Φ_s | Solid's volume fraction original fluid |
| Φ_f | Solid's volume fraction filter cake |
| ε | Void fraction equivalent to surface porosity |
| ρ | Density |
| A_{pigment} | Pigment area |
| A_{total} | Total area |
| A_{void} | Pore area |

Initially the Lucas Washburn equation was used to describe the ink vehicle uptake by paper. Based on the Lucas Washburn equation shown in Eq. 1, the distance travelled by the liquid front in the tube is a function of the elapsed time, the fluid viscosity, the interfacial tension and the contact angle between the fluid and the capillary pore radius.

$$\text{Eq. 1} \quad x^2 = \frac{R \cdot \gamma \cdot \cos \theta \cdot t}{2 \cdot \eta}$$

$$\text{Eq. 2} \quad V_p = n_p \cdot \pi \cdot R^2 \cdot \sqrt{\frac{R \cdot \gamma \cdot \cos \theta \cdot t}{2 \cdot \eta}}$$

Eq. 2 shows that based on the Lucas-Washburn equation, a large number of coarse pores gives highest penetration volume and consequently fastest ink vehicle uptake.

SCHÖLKOPF [6] compared the penetration models of Lucas Washburn and Bosanquet in detail. The main drawback of the Lucas-Washburn approach was that it neglected the inertia of the penetrating fluid. Bosanquet added the inertia impulse drag effect associated with an accelerated fluid, based on following force balance:

$$\text{Eq. 3} \quad F_i + F_{vd} = F_p + F_w$$

F_w is the inertial force according to Newton's second law, and equals $d(mdx/dt)/dt$, where m is the mass of the fluid in the capillary ($=\pi R^2 \rho x$) and mdx/dt is the momentum, or inertia, of the fluid. F_{vd} is the force due to viscous drag and follows Poiseuille's law. F_p is the force acting by an external pressure p_e and F_w is the wetting force. When the terms are brought in their dynamic form, one obtains the following Bosanquet relation:

$$\text{Eq. 4} \quad \frac{d}{dt} \left(\pi \cdot R^2 \cdot \rho \cdot x \frac{dx}{dt} \right) + 8 \cdot \pi \cdot \eta \cdot x \frac{dx}{dt} = p_e \cdot \pi \cdot R^2 + 2 \cdot \pi \cdot R \cdot \gamma \cdot \cos \theta$$

For the case that the starting point is zero and no external pressure is applied, the distance travelled by the liquid front in the tube can be calculated:

$$\text{Eq. 5} \quad x^2 = \frac{2 \cdot \gamma \cdot \cos \theta \cdot t^2}{R \cdot \rho} \quad (t \ll 1, p_e = 0)$$

$$\text{Eq. 6} \quad V_p = n_p \cdot \pi \cdot R^2 \cdot \sqrt{\frac{2 \cdot \gamma \cdot \cos \theta \cdot t^2}{R \cdot \rho}} = \varepsilon \cdot \sqrt{\frac{2 \cdot \gamma \cdot \cos \theta \cdot t^2}{R \cdot \rho}} \quad (t \ll 1, p_e = 0)$$

Based on Eq. 5, smaller pores lead to faster liquid uptake in a single capillary. SCHÖLKOPF ET AL. [7] demonstrated also, that the proposed Bosanquet flow changes from inertial to Lucas-Washburn flow as time and distance increase. The smaller the pore radius, the faster the change-over will occur.

When the penetration volume per unit area is calculated like shown in Eq. 6, it can be seen that many coarse pores give higher penetration volume. But at constant surface porosity ε (defined as ratio of pore area to total area, see Eq. 13), smaller pores give higher liquid absorption.

PRESTON ET AL. [8, 9] chose a practical approach to describe the role of pore density on ink setting of offset printing ink applied on coated papers. Ink setting rate was studied by measuring the ink tack development of ink printed onto coated papers with a wide range of pore structures. Pore size and pore volume of coated papers were analysed by mercury porosimetry. Based on the assumption that all pores are cylindrical, the pore density per unit area could be calculated. Gathered data confirmed that the Lucas-Washburn model could not be used to describe the ink setting behaviour of offset inks on coated papers. An empirical expression for the total volume of ink vehicle absorbed into the coating structure at a given time was given as:

$$\text{Eq. 7} \quad V_p = n_p \cdot \pi \cdot \sqrt{\frac{R^3 \cdot \gamma \cdot \cos \theta \cdot t}{2 \cdot \eta}}$$

$$\text{Eq. 8} \quad V_p = n_p \cdot \pi \cdot R^2 \cdot \sqrt{\frac{\gamma \cdot \cos \theta \cdot t}{2 \cdot R \cdot \eta}} = \varepsilon \cdot \sqrt{\frac{\gamma \cdot \cos \theta \cdot t}{2 \cdot R \cdot \eta}}$$

Eq. 7 deviates from the simple capillary imbibition model of Lucas-Washburn by a factor $1/R$. Based on Eq. 8 it can be concluded that a large number of coarse pores give highest penetration volume and consequently fastest ink setting – which is in agreement with the finding of SCHÖLKOPF. But also the model presented by PRESTON highlights that at constant surface porosity ε higher liquid absorption can be reached with smaller pores.

XIANG ET AL. [10, 11] published several papers describing the developed filter cake model. In this model, the ink pigment particles and resins are too large to penetrate into the finer coating pores and are filtered out on the surface. Based on performed investigations analysing the coating structure change after printing, the gel layer was able to prevent penetration of pigments into coarse pores.

Based on the developed filter cake equation, the total volume of ink vehicle that is absorbed into the coating structure per unit area was calculated as follows:

$$\text{Eq. 9} \quad V_p = \varepsilon \cdot \sqrt{\frac{R \cdot t \cdot \gamma \cdot \cos \theta}{2 \cdot \eta \cdot \left(1 + \frac{\varepsilon^2 \cdot \phi_s \cdot R^2}{8 \cdot K \cdot \phi_f \cdot (1 - \phi_s)}\right)}}$$

In case of low resistancy of filter cake, or as the filter cake permeability $K \rightarrow \infty$, Eq. 9 is reduced to the well known Lucas-Washburn equation:

$$\text{Eq. 10} \quad V_p = \varepsilon \cdot \sqrt{\frac{R \cdot \gamma \cdot \cos \theta \cdot t}{2 \cdot \eta}}$$

If K is small, which means that the filter cake resistance becomes important, Eq. 9 can be reduced to

$$\text{Eq. 11} \quad V_p = \sqrt{\frac{4 \cdot K \cdot t \cdot \gamma \cdot \phi_f \cdot (1 - \phi_s) \cdot \cos \theta}{R \cdot \eta \cdot \phi_s}}$$

Based on Eq. 11, the total volume of ink vehicle that was absorbed into the coating structure per unit area is a function of $1/R^{1/2}$. Actually the filter cake model, which takes the resistance of the formed filter cake into account, predicts faster ink setting realised with smaller pores in the coating structure.

The surface porosity of coated papers

For our field of application – the printing process of coated papers – the surface porosity of porous substrates has to be taken into account. By calculation of the dimensionless void fraction, which is equivalent to the surface porosity like presented in Eq. 12, the linkage between the pore size and the number of pores per unit area can be performed:

$$\text{Eq. 12} \quad \text{surface porosity } \varepsilon = n_p \cdot R^2 \cdot \pi$$

Generally the porosity of the coating layer of coated papers is generated by the use of particles. At this point, the interrelation between the pore and the number of pores is estimated based on a theoretical approach with monodisperse, spherical particles:

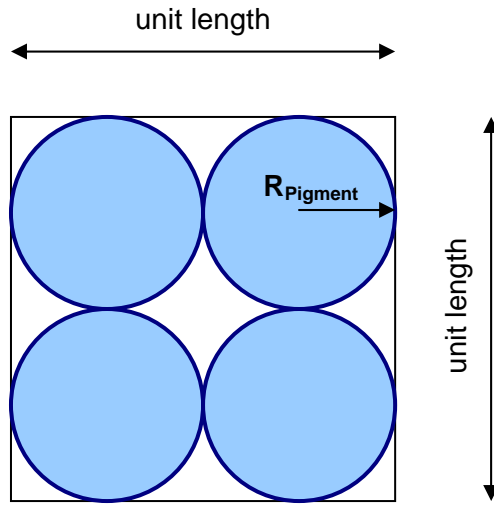


Figure 2 Particle packing of spherical pigments

When the monodisperse pigment particles with the corresponding particle radius $R_{pigment}$ are clustered as demonstrated in *Figure 2*, surface porosity ε can be calculated analytically. It is defined as the ratio of pore area A_{void} to total area A_{total} .

$$\text{Eq. 13} \quad \text{surface porosity } \varepsilon = \frac{\text{Pore Area}}{\text{Total Area}} = \frac{A_{void}}{A_{total}}$$

Pore area A_{void} is the difference between total area A_{total} and pigment area $A_{pigment}$, also $A_{void} = A_{total} - A_{pigment}$. Considering *Figure 2* for pigment area and total area (i.e. unit area) we obtain:

$$\text{Eq. 14} \quad \varepsilon = \frac{A_{void}}{A_{total}} = \frac{A_{total} - A_{pigment}}{A_{total}} = 1 - \frac{4 \cdot R_{pigment}^2 \cdot \pi}{(4 \cdot R_{pigment})^2} = 1 - \frac{\pi}{4} \cong 0.215 = \text{constant}$$

By doing so, the surface porosity of a certain pigment packing is a constant and independent from the pore size and finally by the size from the used particles. Due to this, the number of pores can not be changed independently from the size of the pores.

This theoretical approach describing the surface porosity as a function of the particle size is valid for uncalendered papers. It is expected that the following calendering process leads to alignment and consequently to compression of the initial pore structure. Objective of the following investigation was to analyse the influence of different calendering settings on the compression level of coated papers and consequently on the ink setting behaviour.

PORE STRUCTURE CHANGES DUE TO CALENDERING AND THE EFFECT ON INK SETTING BEHAVIOUR

Due to a low degree of particle alignment after coating application, coated papers typically have a matt or silk surface character. Calendering is widely used as a final step to improve paper gloss and smoothness of the coated papers. In addition to the improvements regarding surface characteristics, calendering leads to decreased pore volume and pore size as a result of the permanent compression of the coating layer. As summarised in this chapter, calendering can lead to undesired changes especially regarding ink setting but also concerning optical aspects like opacity.

KOSSE ET AL. [4] confirmed the reduction of pore volume during calendering and showed that this pore volume reduction of the whole paper can be up to 48% compared to the uncalendered papers. The main part of the pore volume reduction happens in the base paper (fibre matrix), but also the coating layer gets compressed and the typical pore diameter is shifted to smaller pore diameters.

LARSSON ET AL. [12] demonstrated that calendering of coated paper caused a significant change in pore size distribution. Pore volume and pore size are reduced by calendering. It was found that pore volume of pure clay coating is reduced twice as much as those of pure GCC coating. The collapsing of the loose structure built by the platy clay particles during calendering can be limited by addition of 30% of GCC. Calendering of coated papers leads to a denser surface structure with more aligned clay particles as highlighted by HIORNS ET AL. [13]. Based on the shown SEM images, the reduced ink setting behaviour of calendered papers is a result of the lower pore volume of the coating layer and by a clearly denser surface structure with a reduced amount of pores per unit area. Both changes, the dense surface and the reduced pore volume, retard ink vehicle absorption of calendered papers, which was also highlighted by BLUVOL ET AL. [14].

The influence of viscoelastic behaviour of paper coating on the end use performance of coated papers was studied by KAN ET AL. [15]. Higher glossability is realised with coating having high elastic modulus (higher compressibility). The viscoelastic properties of paper coating are generally determined by the viscoelasticity of the used latex and the volume fractions of the pigment, binder and void. Coatings containing plastic pigments have higher uncalendered paper gloss (due to lower shrinkage) and higher glossability at calendering (due to higher void volume in the coating).

Furthermore it was found that an increase of latex content leads to a greater compressibility of the immobilised coating structure. This observation is explained by an improved lubrication of the pigments and the collapse of the bridges under high temperature and high load, see for instance LARSSON ET AL. [16].

The influence of latex on the deformation behaviour of coating structure during calendering was investigated by MIKKILA ET AL. [17]. When hard latex (high T_g) is used, the high stiffness of the coating reduces the ability of the coating to deform. The soft latex (low T_g) restricts the deformation during calendering by the good film forming properties. The coating containing the latex with intermediate T_g can be most easily deformed. Furthermore it is shown that calendering at low temperature influences more the porosity of the coating than the gloss of the coating layer.

The gathered information available in the literature is based on investigations done for different paper grades. Objective of this work is to link the pore structure as well as the surface porosity of coated and calendered papers with the observed ink setting behaviour. A further target was to study, whether the currently available penetration models describing the ink solvent absorption into coating structures are also universally valid in describing the influence of calendering induced pore changes on the ink setting behaviour of the calendered end-paper.

An investigation of the influence of steel roll temperature, number of calender passes as well as line load was performed with a commercial (woodfree) triple coated paper having a grammage of 135 g/m². This calendering series was performed on a standard laboratory calender (Kleinwefers laboratory calender; two roll system consisting of a hard and heated steel roll and a soft woolpaper reel) and was split into 3 parts:

- Series 1: Varied steel roll temperature (25°C, 50°C, 70°C and 90°C) at constant number of passes (10 passes) and constant line load (1000 daN)
- Series 2: Varied number of passes (2, 4, 6 and 10 passes) at constant steel roll temperature (70°C) and constant line load (1000 daN)
- Series 3: Increased line load (1000 and 4000 daN) at constant number of passes (10 passes) and constant steel roll temperature (70°C)

Materials and methods

The following standard properties of the uncalendered paper as well as the calendered papers were analysed:

- Grammage
- Calliper
- Specific volume
- Paper gloss Tappi 75°
- Paper gloss DIN 75°
- Paper gloss DIN 45°
- PPS roughness
- set-off (15, 30, 60 and 120 seconds after printing)

A mercury porosimeter, Autopore IV 9500, from Micromeritics Instrument Corp., was used to characterise the pore structure of the test papers (uncalendered and calendered). The pore structure data were corrected by using the Pore-comp software (University of Plymouth, U.K.).

The surface porosity was analysed by image analysis on a series of SEM images.

Detailed results of the performed investigations are given in the Appendix (tables A1 – A3).

Results and discussion

The mercury porosimetry results (*Figures 3-5*) confirm that the fibre network of the base paper gets permanently compressed during calendaring. A stepwise decrease of characteristic pore diameter is found with increased steel roll temperature (see *Figure 3*). Void volume (porosity) of calendered paper is clearly reduced by increased roll temperature. The influence of calender settings is also visible in the pore diameter range typical for coating layer but not as distinct as for the fibre network.

When the number of passes is changed at constant temperature, the permanent pore structure change is already reached after 4 passes through the laboratory calender (see *Figure 4*), a further increase in the number of passed does not result in any significant further change in the pore structure.

An increase of nip load from 1000 to 4000 daN results in a significantly higher compression of the whole paper as presented in *Figure 5*.

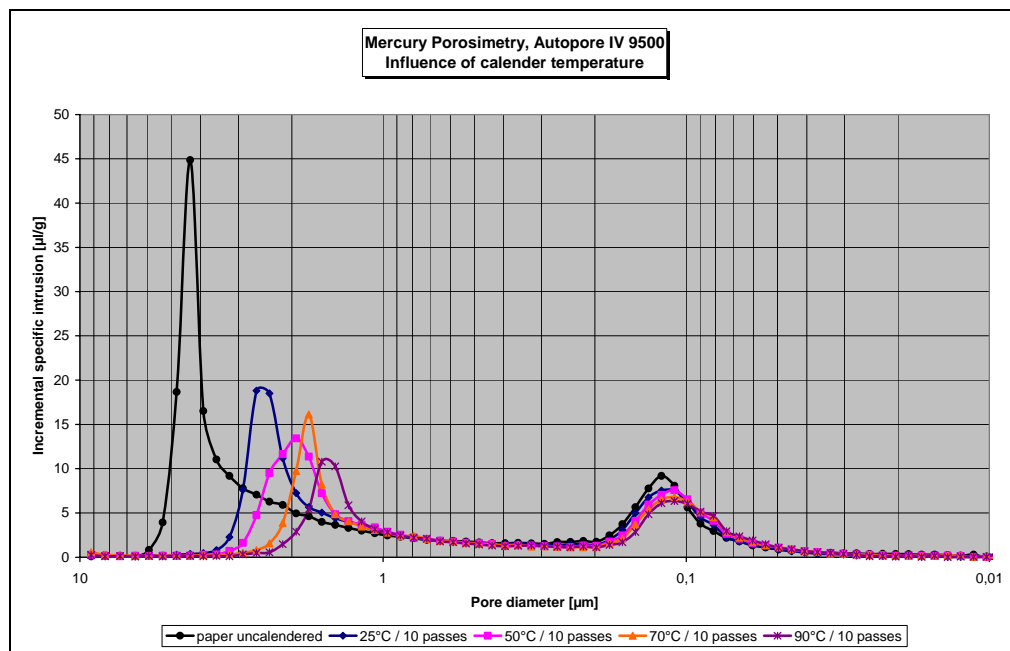


Figure 3 Series 1: The influence of calendaring temperature on pore structure

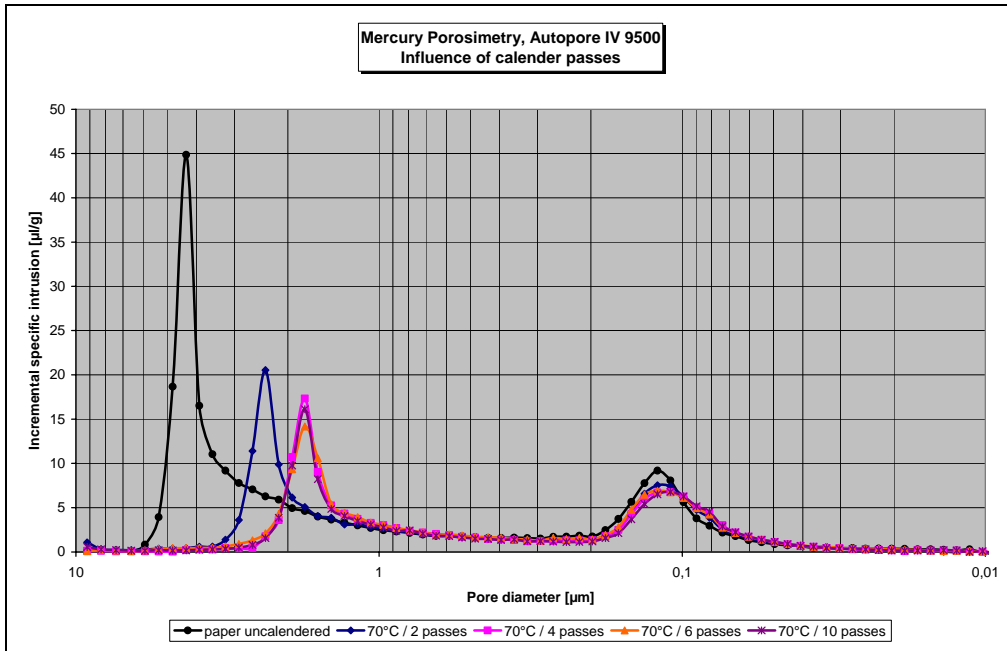


Figure 4 Series 2: The influence of the number of nip passes on pore structure

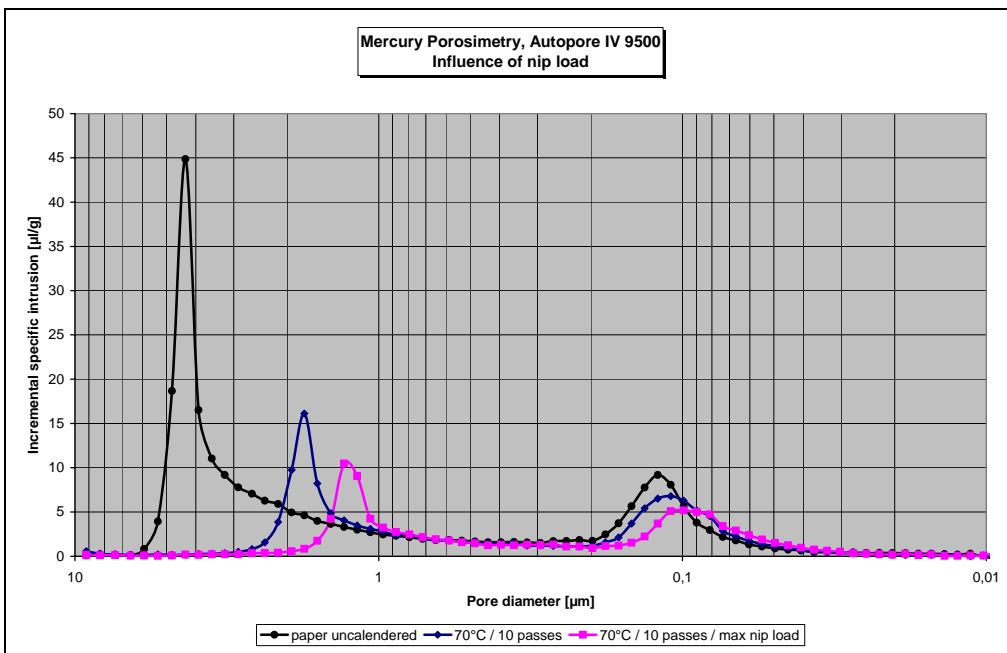


Figure 5 Series 3: The influence of nip load on pore structure

Figure 6 and *Figure 7* show the well-known trend that paper gloss increases with increasing calendering temperature at constant number of passes as well as with increased number of passes at constant calendering temperature. The influence of calendering temperature on paper gloss is higher than the influence of the number of passes. For highest gloss levels, high calendering temperature is essential.

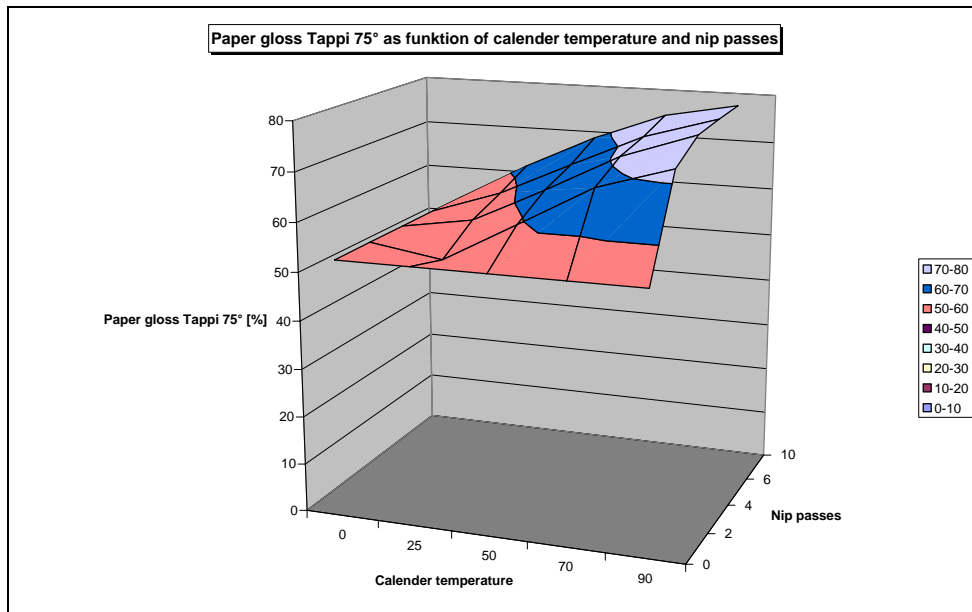


Figure 6 Paper gloss Tappi 75° as a function of calendaring temperature and nip passes (mean of top and wire side)

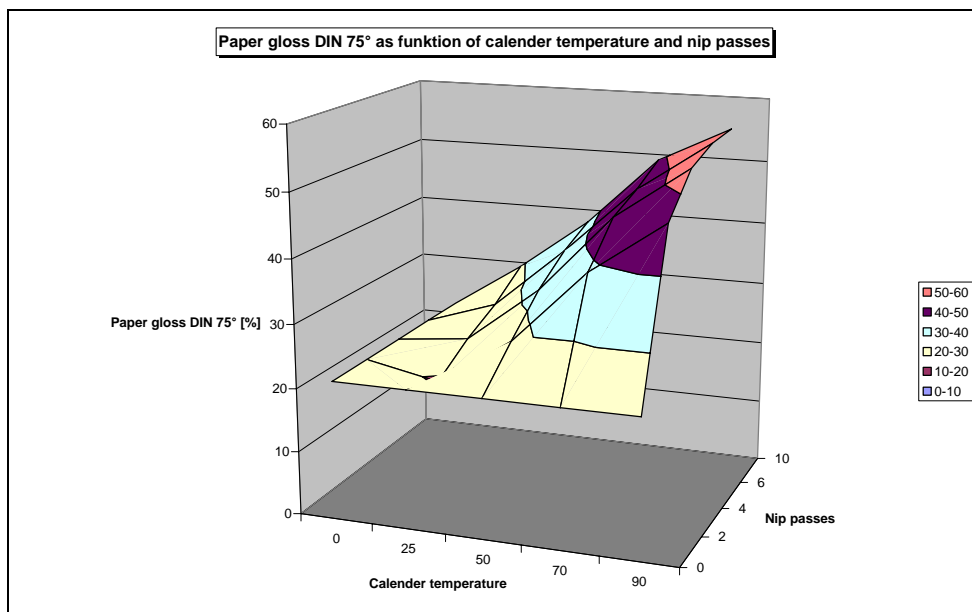


Figure 7 Paper gloss DIN 75° as a function of calendaring temperature and nip passes (mean of top and wire side)

As demonstrated in *Figure 8*, ink setting rate decreases when steel roll temperature is increased. The number of passes through the laboratory calender at constant steel roll temperature showed no significant impact on ink setting rate (see *Figure 9*).

It has to be concluded that the permanent compression of the paper structure leads to significantly slower ink setting. The used temperature dominates the change of pore structure whilst the number of passes has no significant influence.

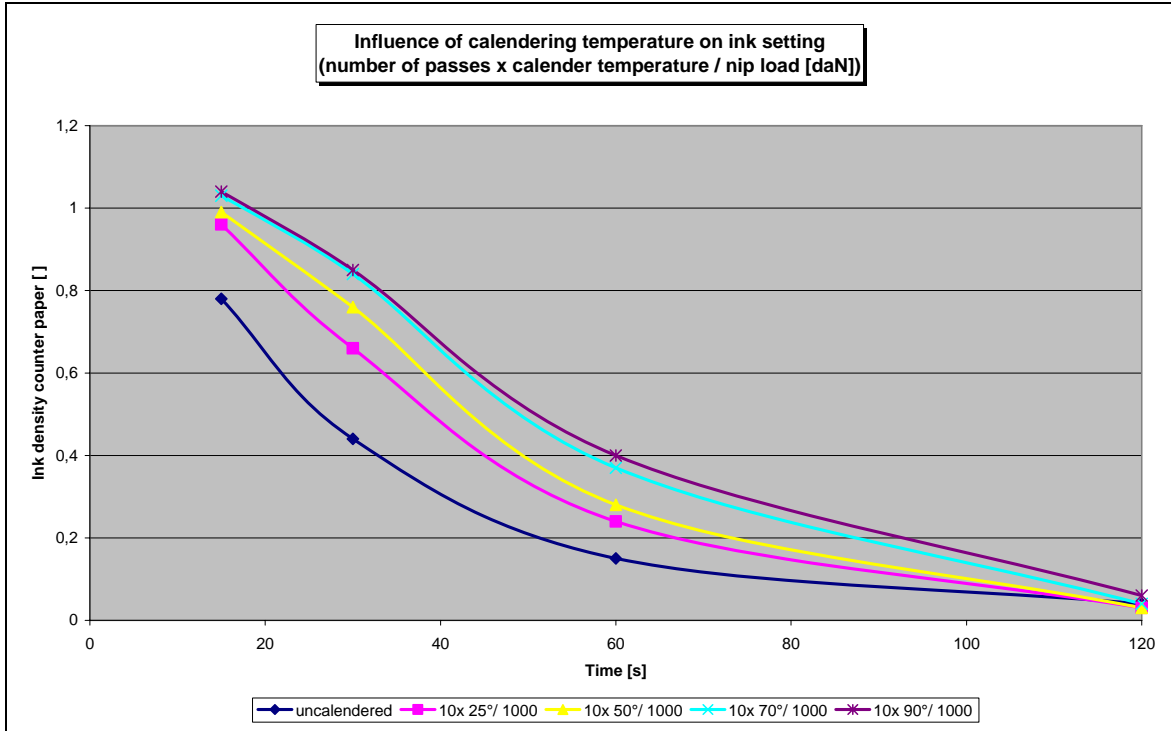


Figure 8 Ink setting as a function of steel roll temperature at calendaring

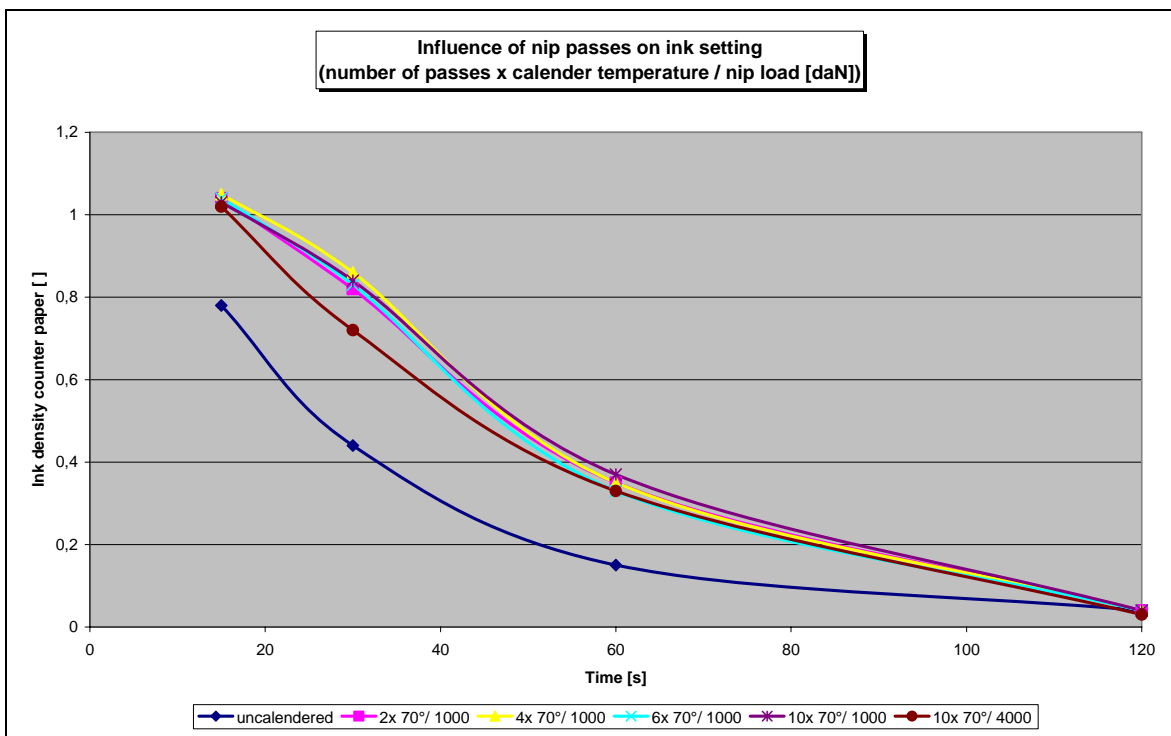


Figure 9 Ink setting as a function of the number of passes through calender

Surface pore size was measured on 5 SEM images per paper sample (total area evaluated per SEM picture was 90 μm^2) acquired at a resolution of 0.01 μm per pixel. A grey level threshold was set manually on each image and all closed image regions darker than the threshold were considered as pores. With this image analysis of the SEM pictures the following surface structure descriptive data were obtained:

- Pore size of each pore
- Perimeter of each pore
- Pore area of each pore
- Total pore area (sum of all pore areas detected)
- Hydraulic diameter of each pore (equivalent to 4 * pore area over pore perimeter)
- Median pore diameter (hydraulic) – 50% of the pores have a pore size smaller than the median pore diameter
- Number of surface pores detected

Table 1 Results of image analysis of SEM pictures (description of the used calendering setting: nip passes * steel roll temperature / nip load)

| | <i>Uncalendered</i> | <i>10*25*/1000</i> | <i>10*50*/1000</i> | <i>10*70*/1000</i> | <i>10*90*/1000</i> |
|--|---------------------|--------------------|--------------------|--------------------|--------------------|
| Number of surface pores [] | 444 | 495 | 328 | 507 | 339 |
| Median pore diameter [μm] | 0,099 | 0,086 | 0,084 | 0,083 | 0,072 |
| Total pore area [μm^2] | 4,45 | 3,60 | 2,48 | 3,30 | 1,72 |

As shown in *Table 1*, the median pore diameter (calculated from the hydraulic diameter) decreased with increasing steel roll temperature. Generally also the total area of the surface pores decreases with increasing temperature of the steel roll temperature – with exception of the paper calendered at 70°C.

When the absolute values of the analysed pore size data are compared, the typical pore size of the surface pores detected via image analysis of the SEM pictures is significantly smaller than the typical pore size results of the performed mercury porosimetry investigations. It seems that the surface pores are in general smaller than the average pore structure of the whole coating layer but also method related deviations can not be ruled out, refer for instance to VYÖRYKKA [18].

The results of this investigation demonstrate that the average pore size of coated papers gets permanently compressed and reduced by calendering. This should be beneficial to improve ink setting but the closing the surface pores dominates (leading to lower surface porosity ε) and actually slower ink setting behaviour is found for calendered papers.

The observed phenomenon can be explained by a more dense paper surface, which is a result of the increased film forming of latex at the paper surface as well as the enforced alignment of the coating layer.

The influence of pore structure on ink setting of papers from these calendering trials can be explained by the above discussed Eq. 6 and Eq. 8, which are also valid for this application:

$$\text{Eq. 6a } V_p = n_p \cdot \pi \cdot R^2 \cdot \sqrt{\frac{2 \cdot \gamma \cdot \cos \theta \cdot t^2}{R \cdot \rho}} = \varepsilon \cdot \sqrt{\frac{2 \cdot \gamma \cdot \cos \theta \cdot t^2}{R \cdot \rho}} \quad (t \ll 1, p_e = 0)$$

$$\text{Eq. 8a } V_p = n_p \cdot \pi \cdot R^2 \cdot \sqrt{\frac{\gamma \cdot \cos \theta \cdot t}{2 \cdot R \cdot \eta}} = \varepsilon \cdot \sqrt{\frac{\gamma \cdot \cos \theta \cdot t}{2 \cdot R \cdot \eta}}$$

Consequently paper concepts without calendering are of advantage regarding fast ink setting. If calendering is required to reach the desired paper gloss level, calendering with lower surface temperature and higher number of nip passes is proposed. Still, for high gloss papers high calendering temperature will be necessary to reach the required gloss level, compare *Figure 6* and *Figure 7*.

CONCLUSIONS

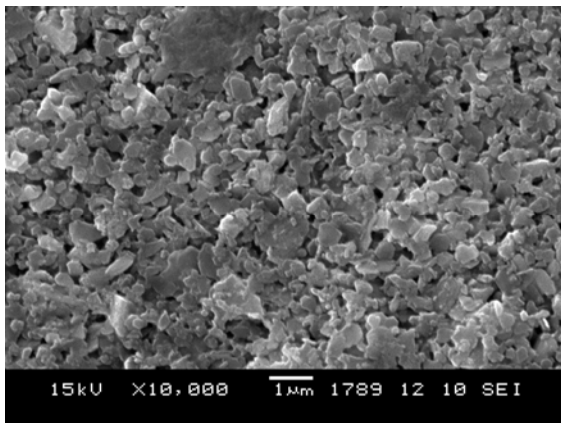
Generally fast ink setting can be realised by use of fine pigments as well as pigments with steep particle size distribution. But this laboratory study clearly demonstrates that the ink-paper interaction of coated papers changes significantly by calendering too.

Observed results demonstrate that pore size of coated papers on average gets permanently compressed and reduced by calendering. Mercury porosimetry and image analysis of SEM pictures highlighted that the gradual reduction of total pore volume in combination with reduced surface porosity results actually in slower ink setting behaviour of papers calendered at higher temperature.

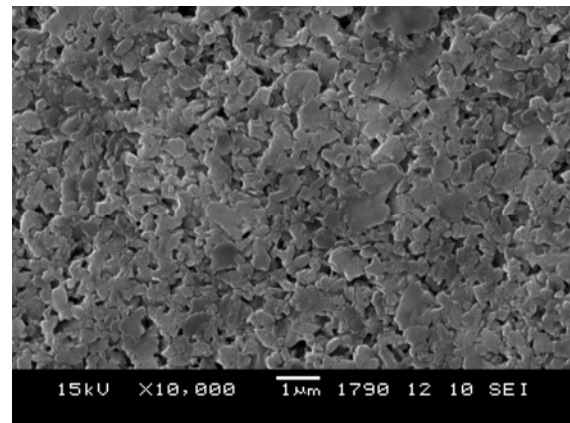
The trend towards smaller pores should theoretically be beneficial to improve ink setting but the closing of surface pores dominates and actually results in slower ink setting behaviour of calendered papers. This observed phenomenon can be explained by a denser coating surface, which is a result of the increased film forming of latex on the surface as well as the enforced alignment of the coating layer.

Despite all the weaknesses of currently available models, they provide the necessary fundamental knowledge on ink and paper interaction. As highlighted, they can also be used to explain the observed slower ink setting behaviour of calendered papers compared to uncalendered papers.

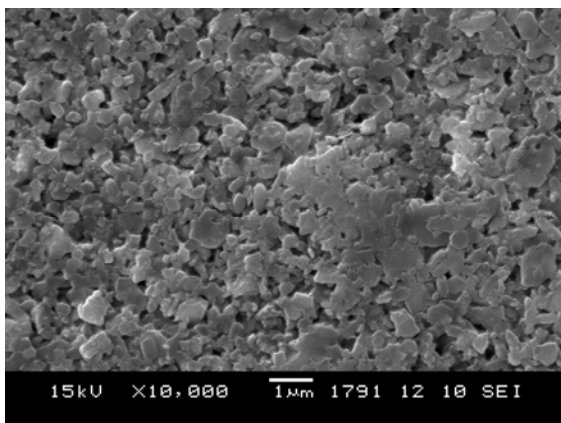
APPENDIX



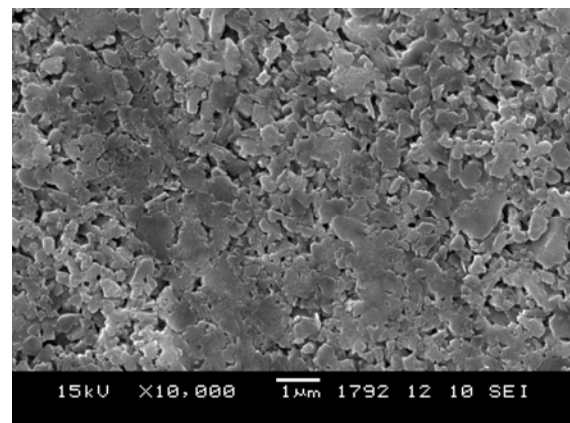
Uncalendered paper



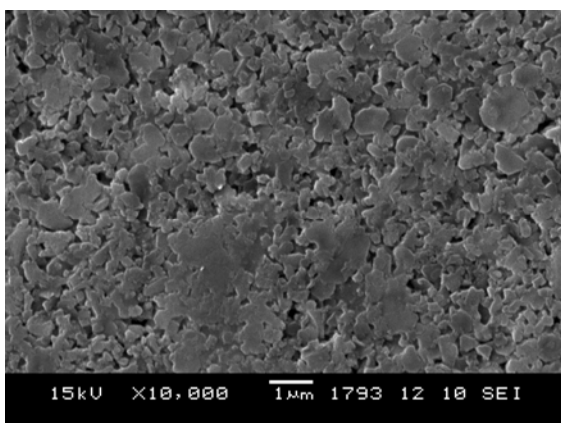
10 * 25°C / 1000 daN



10 * 50°C / 1000 daN



10 * 70°C / 1000 daN



10 * 90°C / 1000 daN

Figure A1 SEM pictures of the laboratory calendered papers (nip passes * steel roll temperature / line load) – magnification of the SEM pictures 10,000:1

Table A1 Analysed paper properties of uncalendered as well as calendered papers:

| calender setting | | uncalendered | 2° 25°/1000 | 4° 25°/1000 | 6° 25°/1000 | 10° 25°/1000 | 2° 50°/1000 | 4° 50°/1000 | 6° 50°/1000 | 10° 50°/1000 |
|---------------------------------|--------------------|--------------|-------------|-------------|-------------|--------------|-------------|-------------|-------------|--------------|
| grammage | g/m ² | 135 | 135 | 135 | 135 | 135 | 135 | 135 | 135 | 135 |
| specific volume | cm ³ /g | 0,83 | 0,77 | 0,75 | 0,76 | 0,75 | 0,74 | 0,72 | 0,72 | 0,73 |
| caliper | mm | 0,112 | 0,104 | 0,102 | 0,102 | 0,102 | 0,1 | 0,098 | 0,098 | 0,098 |
| paper gloss Tappi 75° top side | % | 54,2 | 65,8 | 69,2 | 71,9 | 74,1 | 71,1 | 73,7 | 75,7 | 77,7 |
| paper gloss Tappi 75° wire side | % | 52,1 | 35,9 | 42,1 | 44,7 | 48,7 | 47,4 | 52,4 | 55,3 | 59,6 |
| paper gloss DIN 75° top side | % | 23,7 | 32,2 | 37,4 | 40,7 | 44,8 | 43,9 | 50,8 | 54,6 | 56,4 |
| paper gloss DIN 75° wire side | % | 19,9 | 6,8 | 8,7 | 10,6 | 13,8 | 10,3 | 13,4 | 16,7 | 19,5 |
| paper gloss DIN 45° top side | % | 3,6 | 6,3 | 7,5 | 9 | 12,3 | 9,9 | 13 | 14,8 | 17,6 |
| paper gloss DIN 45° wire side | % | 3,11 | 64,1 | 67,6 | 69,4 | 73,2 | 69,9 | 73,3 | 74,4 | 75,5 |
| mean Tappi 75° | % | 53,15 | 50,85 | 55,65 | 58,3 | 61,4 | 59,25 | 63,05 | 65,5 | 68,65 |
| mean DIN 75° | % | 21,8 | 19,5 | 23,05 | 25,65 | 29,3 | 27,1 | 32,1 | 35,65 | 37,95 |
| mean DIN 45° | % | 3,355 | 35,2 | 37,55 | 39,2 | 42,75 | 39,9 | 43,15 | 44,6 | 46,55 |
| roughness PPS top side | µm | 1,54 | 0,98 | 0,86 | 0,83 | 0,76 | 0,78 | 0,71 | 0,66 | 0,6 |
| roughness PPS wire side | µm | 1,8 | 1,2 | 1,05 | 0,98 | 0,88 | 0,92 | 0,84 | 0,76 | 0,7 |
| Set-off 15s top side | | 0,78 | | | | 0,96 | | | | 0,99 |
| Set-off 30s top side | | 0,44 | | | | 0,66 | | | | 0,76 |
| Set-off 60s top side | | 0,15 | | | | 0,24 | | | | 0,28 |
| Set-off 120s top side | | 0,04 | | | | 0,03 | | | | 0,03 |

Table A2 Analysed paper properties of uncalendered as well as calendered papers:

| calender setting | | uncalendered | 2° 70°/1000 | 4° 70°/1000 | 6° 70°/1000 | 10° 70°/1000 | 2° 70°/4000 | 4° 70°/4000 | 6° 70°/4000 | 10° 70°/4000 |
|---------------------------------|--------------------|--------------|-------------|-------------|-------------|--------------|-------------|-------------|-------------|--------------|
| grammage | g/m ² | 135 | 135 | 135 | 135 | 135 | 135 | 135 | 135 | 135 |
| specific volume | cm ³ /g | 0,83 | 0,72 | 0,70 | 0,70 | 0,69 | 0,68 | 0,68 | 0,68 | 0,67 |
| caliper | mm | 0,112 | 0,097 | 0,095 | 0,094 | 0,093 | 0,092 | 0,091 | 0,091 | 0,09 |
| paper gloss Tappi 75° top side | % | 54,2 | 74,4 | 77,4 | 78,8 | 80 | 82,7 | 84,7 | 85,9 | 86,8 |
| paper gloss Tappi 75° wire side | % | 52,1 | 61,1 | 64,6 | 66 | 69 | 71,7 | 75,5 | 78,2 | 78,2 |
| paper gloss DIN 75° top side | % | 23,7 | 60,1 | 67 | 68,7 | 70,9 | 72 | 76,6 | 78,3 | 80,5 |
| paper gloss DIN 75° wire side | % | 19,9 | 17,4 | 22 | 24,3 | 27,3 | 31,1 | 37,8 | 41,8 | 43,7 |
| paper gloss DIN 45° top side | % | 3,6 | 19,5 | 24,4 | 26,2 | 30,3 | 33,2 | 40,7 | 43,8 | 46,8 |
| paper gloss DIN 45° wire side | % | 3,11 | 76,5 | 78,4 | 79,1 | 80,6 | 83,9 | 85,8 | 86,5 | 87,6 |
| mean Tappi 75° | % | 53,15 | 67,75 | 71 | 72,4 | 74,5 | 77,2 | 80,1 | 82,05 | 82,5 |
| mean DIN 75° | % | 21,8 | 38,75 | 44,5 | 46,5 | 49,1 | 51,55 | 57,2 | 60,05 | 62,1 |
| mean DIN 45° | % | 3,355 | 48 | 51,4 | 52,65 | 55,45 | 58,55 | 63,25 | 65,15 | 67,2 |
| roughness PPS top side | µm | 1,54 | 0,59 | 0,64 | 0,53 | 0,51 | 0,58 | 0,47 | 0,45 | 0,47 |
| roughness PPS wire side | µm | 1,8 | 0,65 | 0,57 | 0,54 | 0,53 | 0,56 | 0,51 | 0,47 | 0,42 |
| Set-off 15s top side | | 0,78 | 1,04 | 1,05 | 1,04 | 1,03 | | | | 1,02 |
| Set-off 30s top side | | 0,44 | 0,82 | 0,86 | 0,83 | 0,84 | | | | 0,72 |
| Set-off 60s top side | | 0,15 | 0,35 | 0,35 | 0,33 | 0,37 | | | | 0,33 |
| Set-off 120s top side | | 0,04 | 0,04 | 0,04 | 0,04 | 0,04 | | | | 0,03 |

Table A3 Analysed paper properties of uncalendered as well as calendered papers:

| calender setting | | uncalendered | 2° 90°/1000 | 4° 90°/1000 | 6° 90°/1000 | 10° 90°/1000 |
|---------------------------------|--------------------|--------------|-------------|-------------|-------------|--------------|
| grammage | g/m ² | 135 | 135 | 135 | 135 | 135 |
| specific volume | cm ³ /g | 0,83 | 0,70 | 0,69 | 0,69 | 0,69 |
| caliper | mm | 0,112 | 0,094 | 0,093 | 0,092 | 0,092 |
| paper gloss Tappi 75° top side | % | 54,2 | 77,3 | 79,8 | 81,4 | 81,2 |
| paper gloss Tappi 75° wire side | % | 52,1 | 67,6 | 72,8 | 72,6 | 73,6 |
| paper gloss DIN 75° top side | % | 23,7 | 70,7 | 76,3 | 78,3 | 78,4 |
| paper gloss DIN 75° wire side | % | 19,9 | 23,3 | 29,2 | 30,8 | 31,3 |
| paper gloss DIN 45° top side | % | 3,6 | 28,7 | 37,1 | 37,9 | 38,7 |
| paper gloss DIN 45° wire side | % | 3,11 | 80,9 | 83,6 | 83,5 | 83,9 |
| mean Tappi 75° | % | 53,15 | 72,45 | 76,3 | 77 | 77,4 |
| mean DIN 75° | % | 21,8 | 47 | 52,75 | 54,55 | 54,85 |
| mean DIN 45° | % | 3,355 | 54,8 | 60,35 | 60,7 | 61,3 |
| roughness PPS top side | µm | 1,54 | 0,52 | 0,44 | 0,43 | 0,42 |
| roughness PPS wire side | µm | 1,8 | 0,55 | 0,44 | 0,41 | 0,41 |
| Set-off 15s top side | | 0,78 | | | | 1,04 |
| Set-off 30s top side | | 0,44 | | | | 0,85 |
| Set-off 60s top side | | 0,15 | | | | 0,4 |
| Set-off 120s top side | | 0,04 | | | | 0,06 |

REFERENCES

- [1] FOGRA [2007], 'Annual report 2006', Fogra Forschungsgesellschaft Druck e.V., Munich (Germany).
- [2] Resch P. [2001], 'Pore structure analysis of coated papers by use of mercury porosimetry and the influence of pore structure on printability', Diploma thesis, Graz University of Technology.
- [3] Resch P. and Bauer W. [2007], 'The influence of coating pigment on pore size distribution of multiple coated papers and its consequences for printability', in *Proceedings of 23rd PTS Coating Conference*, Baden-Baden (Germany), pp. 12.1-12.15.
- [4] Kosse J., Kleemann S., Naydowski C. and Spielmann D. [2003], 'Influence of pigment fineness on pore structure of coated surface' *Wochenblatt für Papierfabrikation* **131**(7), pp. 348-353.
- [5] Donigian D. [2005a], 'The coating-ink interface and the setting of offset printing ink' in *Proceedings of PTS Seminar: Interface Chemistry, PTS*.
- [6] Schölkopf J. [2002], 'Observation and modelling of fluid transport into porous paper coating structures', PhD thesis, University of Plymouth (England).
- [7] Schölkopf J., Gane P. and Ridgway C. [2000], 'Influence of inertia on liquid absorption into paper coating structures', *Nordic Pulp and Paper Research Journal* **15**(5), pp. 422-430.
- [8] Preston J. [2001], 'The influence of coating structure on the print gloss of coated paper surfaces', PhD thesis, University of Bristol (England).
- [9] Preston J., Elton N., Legrix A., Nutbeem C. and Husband J. [2002], 'The role of pore density in the setting of offset printing ink on coated paper', *Tappi Journal*, pp. 3-5.
- [10] Xiang Y. and Bousfield D. [2000], 'Influence of coating structure on ink tack dynamics', *Journal of Pulp and Paper Science* **26**(6), pp. 221-227.
- [11] Xiang Y., Bousfield D., Hayes P. and Kettle J. [2004], 'A model to predict ink-setting rates based on pore-size distributions', *Journal of Pulp and Paper Science* **30**(5), pp. 117-120.
- [12] Larsson M., Vidal D., Engström G., Lepoutre P. and Zou X. [2005], 'Paper coating properties as affected by pigment blending and calendering - an experimental study', in *Proceedings of 22nd PTS Coating Symposium*, Baden-Baden (Germany), PTS, pp. 24.1-24.16.
- [13] Hiorns A., Elton J., Coggan L. and Parsons D. [1998], 'Analysis of differences in coating structure induced through variable calendering conditions', in *Proceedings of Coating and Papermakers Conference*, New Orleans (USA), Tappi Press, pp. 583-602.
- [14] Bluvol G., Burri P., Carlsson R. and Salminen P. [2003], 'Optimising ink setting for double coated wood-free papers', in *Proceedings of 21st PTS Coating Symposium*, Baden-Baden (Germany), PTS, pp. 17.1-17.17.
- [15] Kan C., Kim L., Lee D. and Van-Gilder R. [1997], 'Viscoelastic properties of paper coatings: relationship between coating structure-viscoelasticity and end-use performance', *Tappi Journal* **80**(5), pp. 191-201.
- [16] Larsson M., Engström G., Vidal D. and Zou X. [2006], 'Compression of coating structure during calendering', in *Proceedings of 9th Tappi Advanced Coating Fundamentals Symposium*, Turku (Finland), Tappi Press.
- [17] Mikkilä J., Jarvinen H., Starck P., Lahelin M. and Lofgren B. [2002], 'Deformation of coating layer in calendering', *Wochenblatt für Papierfabrikation* **130**(20), pp. 1328-1332.
- [18] Vyörykkä J., Fogden A., Daicic J., Ernstsson M. and Jääskeläinen A.. [2006], 'Characterization of paper coatings – review and future possibilities', in *Proceedings of 9th Tappi Advanced Coating Fundamentals Symposium*, Turku (Finland), Tappi Press.